Supporting Information

Pressure-Engineered Trap-Controlled Multimodal Luminescence for Versatile Emission Responses in Pr-doped $NaNbO_3$

Tingting Zhao, [a] Hao Wang, [a] Mei Li, [a] Shang Peng, [a] Bohao Zhao, [a] Qi Feng, [a] Yanlong Chen, [a] Yingxue Han, [a] Jun Yuan, [a] Ningxiao Feng, [a] Jiao An, [a] Sheng Jiang*[b] and Chuanlong Lin*[a]

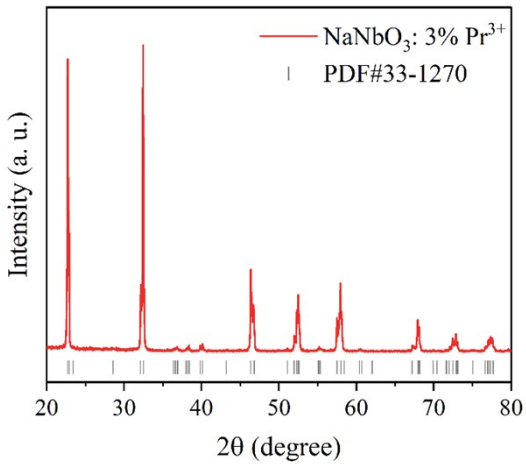

Figure S1 XRD pattern of $NaNbO_3$: 3%Pr^{3+} phosphors.

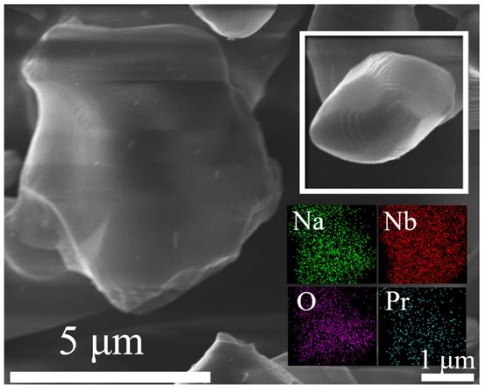

Figure S2 SEM image and elemental mappings of $NaNbO_3$: 3%Pr^{3+}.

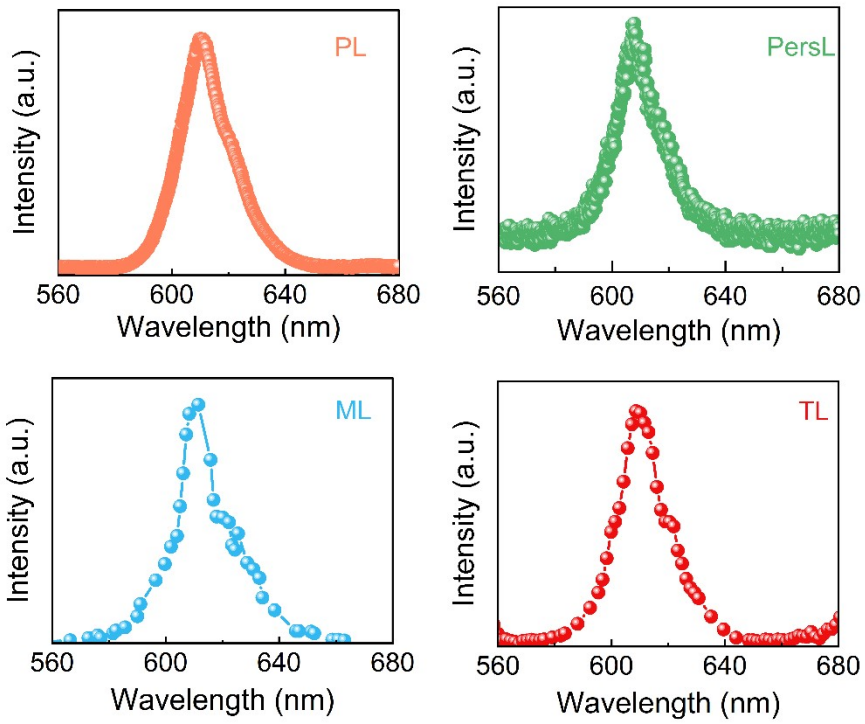

Figure S3 The PL, PersL, ML and TL emission spectra.

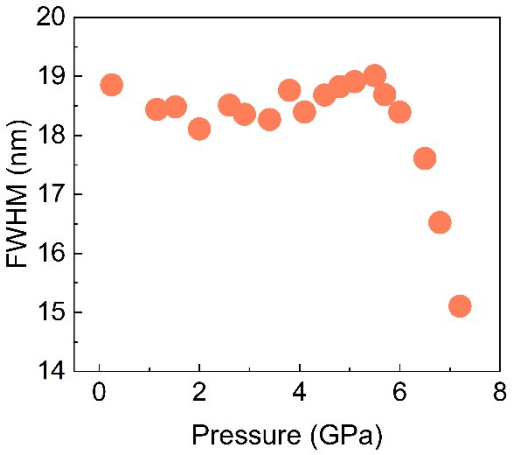

Figure S4 FWHM of $NaNbO_3$: 3%Pr^{3+} phosphors as a function of pressure.

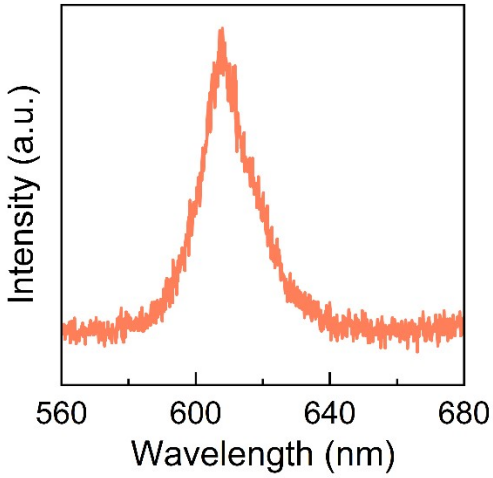

Figure S5 PersL spectrum of $NaNbO_3$: 3%Pr^{3+} phosphors when pre-irradiated with a 405 nm laser for 5 minutes.

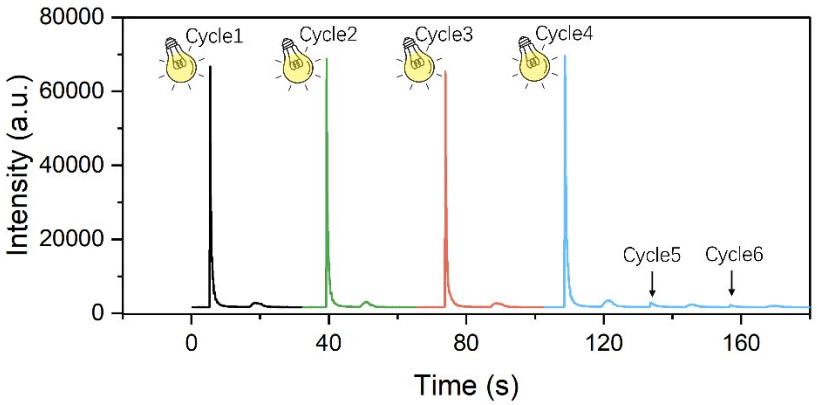

Figure S6 Recoverability of ML after UV light irradiation. Cycles 1-4 were each subjected to 405 nm laser irradiation for 5 min before measurement, while Cycles 5 and 6 were recorded without additional irradiation.

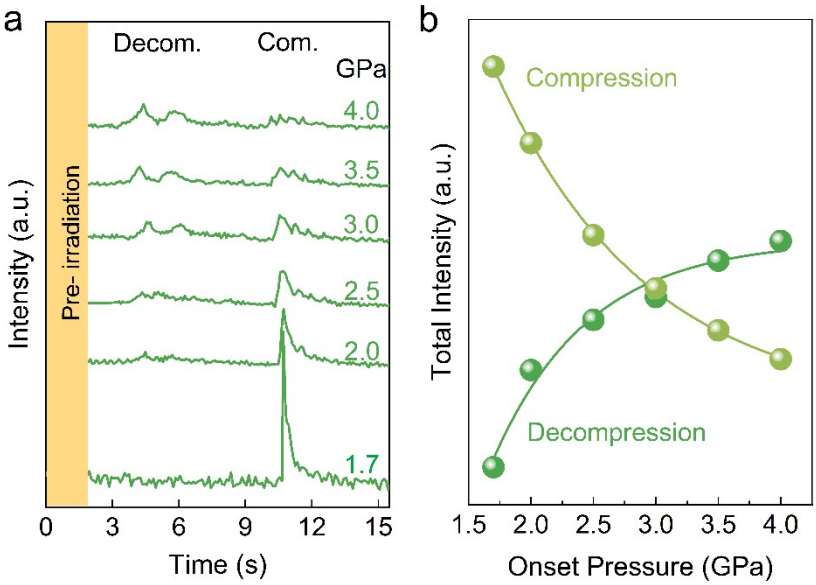

Figure S7 (a) Time-dependent ML intensity during the decompression-compression circle after pre-irradiation by the 405 nm laser under various P_{onset}. The ML signals were collected during decompression from different onset pressure (P_{onset}) to ambient pressure and then during compression from ambient pressure to ~11 GPa, i.e., P_{onset}→ ambient pressure→11.0 GPa) (b) Integrated ML intensities as a function of P_{onset} for the compression and decompression processes.

Considering the significant influence of pressure on ML intensity, we designed a controlled experiment to determine whether the reduction in ML intensity is directly attributable to pressure range. Figure S7a illustrates the ML dynamic behavior of the sample under a constant compression rate after being charged at different P_{onset}, followed by pressure release to ambient pressure and then compression up to 11.0 GPa. During the decompression process, the ML behavior becomes more pronounced with increasing P_{onset}, exhibiting two broad intensity peaks with time. In contrast, during the compression process, the ML behaviour becomes progressively attenuated with increasing P_{onset}. Quantitative analysis of the integrated ML intensities, as shown in Figure S7b, reveals distinct exponential behaviors for the two processes: the compression process follows a single-exponential decay, while the decompression process exhibits a single-exponential increase. Notably, at P_{onset} between 1.5 and 3.0 GPa, the total ML intensity during compression exceeds that observed during decompression. However, as the pressure increases to 3.0-7.4 GPa, the decompression process gradually becomes the dominant pathway for electron release. Identical luminescence behavior during compression process was observed in both types of pressurization experiments, regardless of whether the pressure was increased incrementally from 0.7 GPa or applied directly from the P_{onset} pressure to 11.0 GPa. This consistency implies that the phenomenon is predominantly determined by the initial charging pressure, rather than the pressure range.

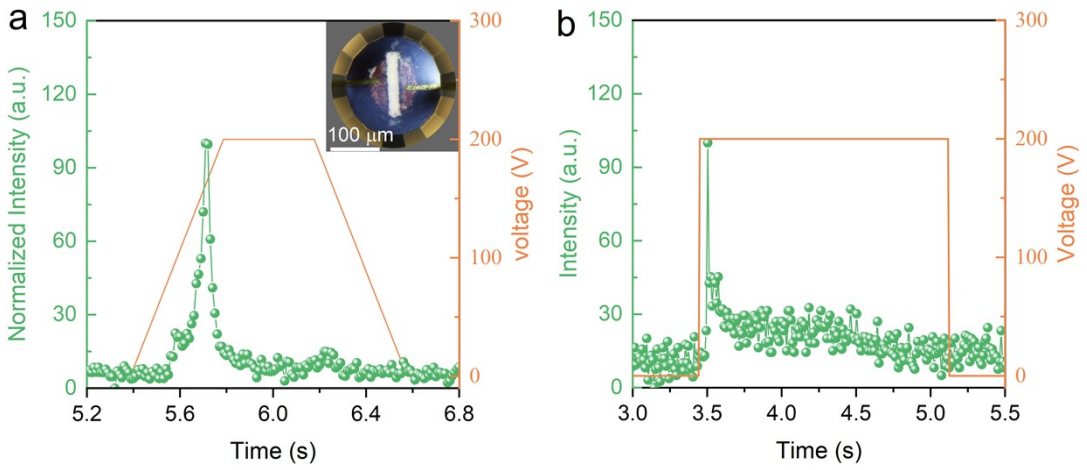

Figure S8 EL spectra at (a) trapezoidal wave and (b) square wave pulse voltages. The insert schematic drawing of arrangement of sample $NaNbO_3$:Pr^{3+} and electrode in DAC for high pressure experiments.

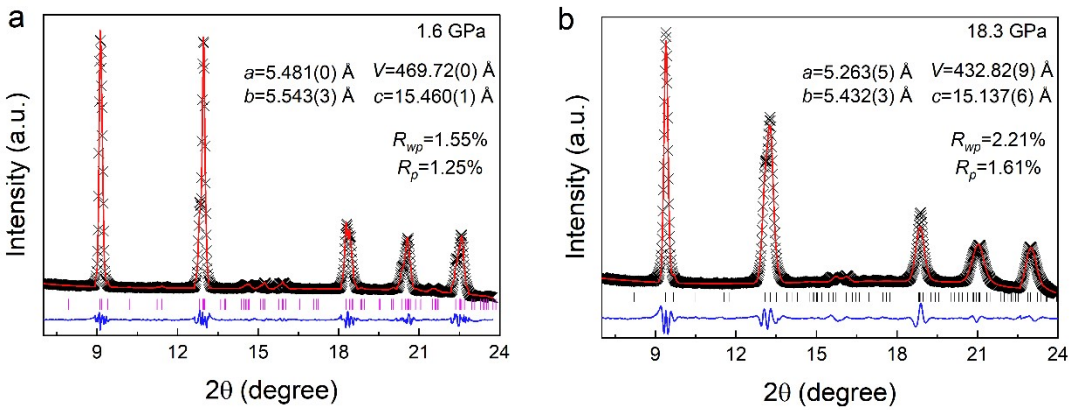

Figure S9 Refinement of the XRD pattern of $NaNbO_3$:Pr^{3+} at (a) 1.6 GPa and (b) 18.3 GPa.

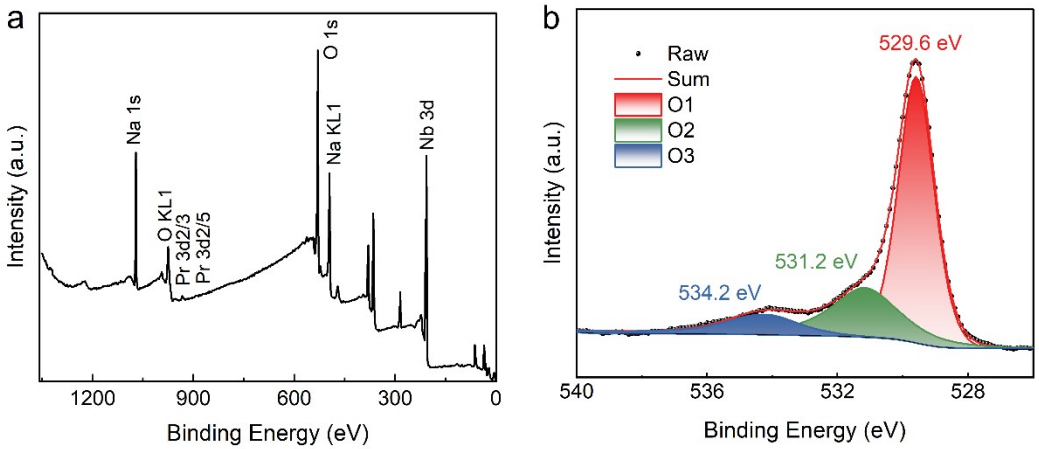

Figure S10 (a) XPS spectrum and (b) Fitted O1s XPS spectrum of $NaNbO_3$: Pr^{3+}.

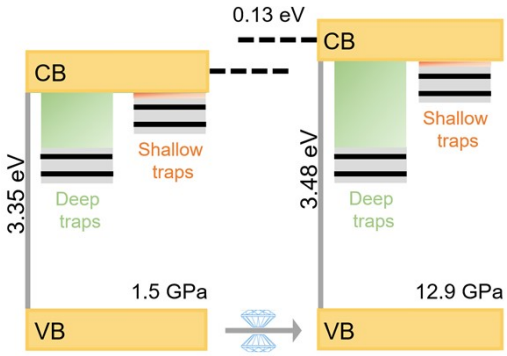

Figure S11 A schematic band structure diagram showing relative trap levels at 1.5 and 12.9 GPa.

Video: Microscopic optical videos of PL, PersL, and ML emissions from $NaNbO_3:Pr^{3+}$ under different P_{onset}.


0.6.mp4


0.8.mp4


1.1.mp4


2.0.mp4


3.0.mp4


4.0.mp4